A first-principles method to calculate fourth-order elastic constants of solid materials

Abhiyan Pandit[a], Angelo Bongiorno[a,b,*]

[a] *Department of Chemistry, College of Staten Island, Staten Island, NY 10314, USA*
[b] *The Graduate Center of the City University of New York, New York, NY 10016, USA*

Abstract

A *first-principles* method is presented to calculate elastic constants up to the fourth order of crystals with the cubic and hexagonal symmetries. The method relies on the numerical differentiation of the second Piola-Kirchhoff stress tensor and a density functional theory approach to calculate the Cauchy stress tensor for a list of deformed configurations of a reference state. The number of strained configurations required to calculate the independent elastic constants of the second, third, and fourth order is 24 and 37 for crystals with the cubic and hexagonal symmetries, respectively. Here, we present conceptual aspects of our method, we provide technical details of its implementation and use, we assess its accuracy, and we discuss several applications. In particular, this method is applied to five crystalline materials with the cubic symmetry (diamond, silicon, aluminum, silver, and gold) and two metals with the hexagonal close packing structure (beryllium and magnesium). Our results are compared to available experimental data and previous computational studies. Calculated linear and nonlinear elastic constants are also used in the context of nonlinear elasticity theory to predict values of volume and bulk modulus over an interval of pressures. These predictions are compared to results obtained from density functional theory calculations to assess the reliability of our method.

Keywords: Density functional theory; nonlinear elasticity; second Piola-Kirchhoff stress tensor; finite differentiation; third-order elastic constants; fourth-order elastic constants; *xPK2x* program

1. Introduction

The elastic constants of a material define the relationship between stress and applied strain [1]. The linear coefficients in this relationship correspond to the second-order elastic constants (SOECs) [1]. These linear coefficients are related to the elastic moduli of a material and are important, for example, to quantify the linear response to a deformation [1], and to calculate the speed of sound waves [1]. The techniques to measure and calculate SOECs are well established, and in fact these coefficients are known for a broad class of materials [2]. Nonlinear elastic constants characterize the anharmonic elastic behavior of a material, and they are of both fundamental and practical importance as they govern how thermoelastic properties change with temperature and pressure [1, 3, 4]. The experimental determination of these nonlinear elastic coefficients is challenging [5, 6], and computational methods are needed to predict the values of these materials parameters [7–15]. In this work, we present a new method to calculate from *first principles* elastic constants of a material up to the fourth order.

The isothermal third-order elastic constants (TOECs) correspond to the first-order anharmonic terms in the series expansion of the free energy density of the material with respect to the Green-Lagrangian strain [1]. These elastic coefficients characterize the nonlinear elastic behavior of a material, and they are related to materials properties such as the long-wavelength phonon anharmonicities [16], sound attenuation [17], the thermodynamic Grüneisen parameter [3, 18], thermal expansion and thermal conductivity [19–21], and the intrinsic mechanical strength [1, 22]. TOECs are typically obtained from acoustoelastic experiments [17], wherein sound velocities are measured for a material under different stress conditions [17, 23–25]. These experiments are challenging and subjected to error margins [6], and for this reason, these coefficients are known for a restricted class of materials [10, 26–30].

The conventional approach to calculate TOECs relies on the use of density functional theory (DFT) calculations to construct either energy or stress versus strain curves along a number of deformation modes (see Ref. [31] and references therein). In this approach, the whole set of linear and nonlinear coefficients are then deduced from a nonlinear least-square fitting of the energy-strain or stress-strain relationships [7, 8, 31–35]. The application of this method to materials with the cubic symmetry is straightforward, as the number of independent SOECs and TOECs to be determined is only 3 and 6, respectively. However, for materials with a lower symmetry, this method becomes increasingly cumbersome and less attractive, as demonstrated by the very few number of applications appeared

*Angelo Bongiorno.
angelo.bongiorno@csi.cuny.edu

so far in literature (see Ref. [31] and references therein). An alternative approach to calculate TOECs was proposed very recently by one of the authors [11]. In this method, elastic constants are obtained by combining DFT calculations and a finite deformation approach [2], where each TOEC is calculated independently by second-order numerical differentiation of the second Piola-Kirchhoff (PK2) stress tensor [11]. This method has general applicability, and so far it has been applied to both 2D and 3D materials, with the cubic, hexagonal, and orthorhombic symmetries [4, 11]. Furthermore, recently this method was used in combination with the quasi-harmonic approximation to calculate TOECs at finite temperature [4].

Fourth- and higher-order elastic constants govern the anharmonic regime of a material subjected to large deformations [8, 12, 14, 36, 37]. Knowledge of these higher-order elastic coefficients allows to describe and predict mechanical instability points of a material [13], as well as to characterize the nature of elastic phase transitions [8, 14]. The experimental determination of fourth-order elastic constants (FOECs) is extremely challenging, as large uniaxial stresses need to be applied in acoustoelastic experiments to obtain reliable values of these high-order elastic coefficients [5]. For this reason, to the best of our knowledge, so far FOECs have been measured only for very few materials [5]. DFT calculations have been employed to calculate FOECs [7–10, 12, 14, 15]. In these computational studies, FOECs were obtained by using the approach relying on fitting energy-strain or stress-strain curves. Although straightforward and in principle general, the computational workload and intricacy of this approach increase significantly for low-symmetry materials. Indeed, to the best of our knowledge, to date this approach has been used to calculate FOECs of materials with only the cubic symmetry [7–10, 12, 14].

In this work, we extend the new method developed to calculate TOECs [11] based on finite deformations and numerical differentiation of the PK2 stress tensor to the calculation of FOECs. The most important advantage of the present method over existing approaches is that each nonlinear elastic constant is calculated independently, by considering up to 8 deformed configurations of the reference state. Thanks to this, our method can be easily applied to any material, regardless of its symmetry. Here we apply the method to calculate SOECs, TOECs, and FOECs of five crystalline materials with the cubic symmetry (diamond, silicon, aluminum, silver, and gold), and two materials with the *hcp* structure (magnesium and beryllium).

This manuscript is organized as follows. In Sec. 2, we introduce basic notions of nonlinear elasticity theory, we provide details about the finite difference formulas to calculate SOECs, TOECs, and FOECs, and we discuss technical aspects of the numerical implementation of our methods. In Sec. 3, we present results and discuss the application of our method to the aforementioned materials. Conclusions and outlook are provided in Sec. 4.

2. Methods

2.1. Notions of nonlinear elasticity theory

The Green-Lagrangian strain, μ_{ij}, is defined as [1, 11, 38]:

$$\mu_{ij} = \frac{1}{2}(F_{ki}F_{kj} - \delta_{ij}), \tag{1}$$

where subscript indices refer to Cartesian coordinates, δ_{ij} is the Kronecker delta function, and F_{ij} are components of the deformation gradient. This tensor is defined as:

$$F_{ij} = \frac{\partial x_i}{\partial X_j} \tag{2}$$

where x_i and X_i are the Cartesian coordinates of a material point in the deformed and reference states, respectively. The Helmholtz free energy density, A, can be written as a series expansion in terms of the Lagrangian strain as follows [1, 8, 11, 14, 38]:

$$\begin{aligned} A &= \frac{1}{2}\frac{\partial^2 A}{\partial\mu_{ij}\partial\mu_{lm}}\mu_{ij}\mu_{lm} + \frac{1}{6}\frac{\partial^3 A}{\partial\mu_{ij}\partial\mu_{lm}\partial\mu_{pq}}\mu_{ij}\mu_{lm}\mu_{pq} + \frac{1}{24}\frac{\partial^4 A}{\partial\mu_{ij}\partial\mu_{lm}\partial\mu_{pq}\partial\mu_{rs}}\mu_{ij}\mu_{lm}\mu_{pq}\mu_{rs} + \cdots \\ &= \frac{1}{2}C^{(2)}_{ijlm}\mu_{ij}\mu_{lm} + \frac{1}{6}C^{(3)}_{ijlmpq}\mu_{ij}\mu_{lm}\mu_{pq} + \frac{1}{24}C^{(4)}_{ijlmpqrs}\mu_{ij}\mu_{lm}\mu_{pq}\mu_{rs} + \cdots, \end{aligned} \tag{3}$$

where $C^{(2)}_{ijlm}$, $C^{(3)}_{ijlmpq}$, and $C^{(4)}_{ijlmpqrs}$ are the isothermal SOECs, TOECs, and FOECs of the material in the reference state, respectively. Given a reference state, the PK2 stress tensor, P_{ij}, can be defined in terms of the Helmholtz free energy density, A, as:

$$P_{ij} = \frac{\partial A}{\partial \mu_{ij}}, \tag{4}$$

whereas the relationship between PK2 and Cauchy stress, σ_{ij}, is [1, 4, 11, 38]:

$$\sigma_{ij} = \frac{V}{V'}F_{il}P_{lm}F_{jm}, \tag{5}$$

where V' and V are the volumes of the (same) material points $\vec{x}$ and $\vec{X}$ in the deformed and reference states, respectively. Equations 3 and 4 allow to define the relationship between PK2 stress tensor and linear and nonlinear

elastic constants. Adopting the Voigt notation, this relationship takes the following form:

$$P_\alpha = C^{(2)}_{\alpha\beta}\mu_\beta + \frac{1}{2}C^{(3)}_{\alpha\beta\gamma}\mu_\beta\mu_\gamma + \frac{1}{6}C^{(4)}_{\alpha\beta\gamma\delta}\mu_\beta\mu_\gamma\mu_\delta, \quad (6)$$

where Greek indices run from 1 to 6, and are related to the Cartesian indices pairs as follows: $1 \rightarrow$ xx, $2 \rightarrow$ yy, $3 \rightarrow$ zz, $4 \rightarrow$ yz, $5 \rightarrow$ zx, and $6 \rightarrow$ xy. For sake of completeness, here below we also express the linear and nonlinear elastic constants in terms of the PK2 stress tensor:

$$C^{(2)}_{\alpha\beta} = \frac{\partial P_\alpha}{\partial \mu_\beta}, \quad C^{(3)}_{\alpha\beta\gamma} = \frac{\partial^2 P_\alpha}{\partial \mu_\beta \mu_\gamma}, \quad \text{and} \quad C^{(4)}_{\alpha\beta\gamma\delta} = \frac{\partial^3 P_\alpha}{\partial \mu_\beta \mu_\gamma \mu_\delta}. \quad (7)$$

The present method relies on the definitions above to calculate SOECs, TOECs, and FOECs of a material using a periodic DFT approach. In this work, temperature effects are disregarded and all calculations are carried out in static conditions.

2.2. Finite difference formulas to calculate elastic constants

To calculate SOECs, we use the following central finite difference formula (Eq. 7):

$$C^{(2)}_{\alpha\beta} = \frac{P^{(+\beta)}_\alpha - P^{(-\beta)}_\alpha}{2\xi}, \quad (8)$$

where ξ is a strain parameter, and $P^{(\pm\beta)}_\alpha$ is the α-component of the PK2 stress tensor of a deformed configuration obtained by applying to the reference state a six-dimensional strain vector, $\vec{\mu}$, with the component β equal to $\pm\xi$, and the rest of the components equal to zero. In case of TOECs, we have two different cases. TOECs with at least two out of three indices equal to each other can be calculated using the following second-order central finite difference formula:

$$C^{(3)}_{\alpha\beta\beta} = \frac{P^{(+\beta)}_\alpha + P^{(-\beta)}_\alpha - 2P^{(0)}_\alpha}{\xi^2}, \quad (9)$$

where $P^{(0)}_\alpha$ refers to the α-component of the PK2 stress tensor of the reference state, which is equal to the Cauchy stress tensor. In case of TOECs whose indices are all different, we use the following formula:

$$C^{(3)}_{\alpha\beta\gamma} = \frac{P^{(+\beta,+\gamma)}_\alpha - P^{(-\beta,+\gamma)}_\alpha - P^{(+\beta,-\gamma)}_\alpha + P^{(-\beta,-\gamma)}_\alpha}{4\xi^2}, \quad (10)$$

where $P^{(\pm\beta,\pm\gamma)}_\alpha$ is the α-component of the PK2 stress tensor of a deformed configuration obtained by applying to the reference state a six-dimensional strain vector, $\vec{\mu}$, with components β and γ equal to $\pm\xi$, and the rest of the components equal to zero. In case of FOECs, we have derived the following finite difference formulas to calculate the different types of coefficients:

$$\begin{aligned}
C^{(4)}_{\alpha\beta\beta\beta} &= \frac{P^{(+2\beta)}_\alpha - 2P^{(+\beta)}_\alpha + 2P^{(-\beta)}_\alpha - P^{(-2\beta)}_\alpha}{2\xi^3} \\
C^{(4)}_{\alpha\beta\gamma\gamma} &= \frac{P^{(+\beta,+2\gamma)}_\alpha - P^{(-\beta,+2\gamma)}_\alpha + P^{(+\beta,-2\gamma)}_\alpha - P^{(-\beta,-2\gamma)}_\alpha - 2(P^{(+\beta)}_\alpha - P^{(-\beta)}_\alpha)}{8\xi^3} \\
C^{(4)}_{\alpha\beta\gamma\delta} &= (P^{(+\beta,+\gamma,+\delta)}_\alpha - P^{(+\beta,+\gamma,-\delta)}_\alpha - P^{(+\beta,-\gamma,+\delta)}_\alpha + P^{(+\beta,-\gamma,-\delta)}_\alpha - P^{(-\beta,+\gamma,+\delta)}_\alpha + \\
&\quad + P^{(-\beta,+\gamma,-\delta)}_\alpha + P^{(-\beta,-\gamma,+\delta)}_\alpha - P^{(-\beta,-\gamma,-\delta)}_\alpha)/8\xi^3,
\end{aligned} \quad (11)$$

where $P^{(\pm\beta,\pm\gamma,\pm\delta)}_\alpha$ is the α-component of the PK2 stress tensor of a deformed configuration obtained by applying to the reference state a six-dimensional strain vector, $\vec{\mu}$, with components β, γ, and δ equal to $\pm\xi$, and the rest of the components equal to zero. We remark that the last formula in Eq. 11 has been derived and reported in Ref. [15].

For sake of clarity, we consider the calculation of the two nonlinear elastic constants, $C^{(3)}_{123}$ and $C^{(4)}_{1255}$, of a material with an arbitrary symmetry. Thus, in case of $C^{(3)}_{123}$, we consider the following 4 strain vectors:

$$\begin{aligned}
&(0,+\xi,+\xi,0,0,0),\ (0,-\xi,+\xi,0,0,0), \\
&(0,+\xi,-\xi,0,0,0),\ (0,-\xi,-\xi,0,0,0).
\end{aligned} \quad (12)$$

Each strain vector is used to generate a deformed configuration of the reference state, and the resulting P_1 components of the PK2 stress tensors are then used in Eq. 10 to calculate $C^{(3)}_{123}$. In case of $C^{(4)}_{1255}$, we use the second formula in Eq. 11, with the component P_1 of the PK2 stress tensor resulting from the following 6 deformations:

$$\begin{aligned}
&(0,+\xi,0,0,+2\xi,0),\ (0,-\xi,0,0,+2\xi,0), \\
&(0,+\xi,0,0,-2\xi,0),\ (0,-\xi,0,0,-2\xi,0), \\
&(0,+\xi,0,0,0,0),\ (0,-\xi,0,0,0,0).
\end{aligned} \quad (13)$$

These two examples show that, in contrast to the conventional approach [8, 12–15, 31], our method allows to calculate each nonlinear elastic constant independently, regardless of the symmetry of the material.

2.2.1. SOECs, TOECs, and FOECs of crystals with the cubic or hexagonal symmetry

In this work, we apply our method to materials with the cubic and hexagonal symmetry. A material belonging to the cubic system (point groups: 432, $4\bar{3}m$, and $m\bar{3}m$) has 3, 6, and 11 independent SOECs, TOECs, and FOECs, respectively [1, 8, 36, 37]. To calculate the 3 independent SOECs, we use the following 4 strain vectors:

$$\begin{aligned}&(0,0,0,0,0,0),\ (+\xi,0,0,0,0,0),\\&(-\xi,0,0,0,0,0),(0,0,0,+\xi,0,0,0).\end{aligned}\tag{14}$$

We highlight that, due to the cubic symmetry, $P_4^{(+4)} = -P_4^{(-4)}$, and therefore only one deformation is needed to calculate $C_{44}^{(2)}$. To calculate the 6 independent TOECs, in addition to the deformations in Eq. 14, we use the following 4 strain vectors:

$$\begin{aligned}&(+\xi,+\xi,0,0,0,0),\ (+\xi,-\xi,0,0,0,0),\\&(-\xi,-\xi,0,0,0,0),\ (0,0,0,+\xi,+\xi,0).\end{aligned}\tag{15}$$

Also in this case, the list above excludes strain vectors that lead to redundant deformed states of a material with a cubic symmetry. The 11 independent FOECs are obtained by considering the following 16 additional strain vectors:

$$\begin{aligned}&(+2\xi,0,0,0,0,0),\ (-2\xi,0,0,0,0,0),\\&(+2\xi,+\xi,0,0,0,0),\ (-2\xi,+\xi,0,0,0,0),\\&(+2\xi,-\xi,0,0,0,0),\ (-2\xi,-\xi,0,0,0,0),\\&(+\xi,0,0,+2\xi,0,0),\ (-\xi,0,0,+2\xi,0,0),\\&(+\xi,0,0,0,+2\xi,0),\ (-\xi,0,0,0,+2\xi,0),\\&(0,0,0,+\xi,+\xi,+\xi),\ (0,0,0,-\xi,+\xi,+\xi),\\&(0,0,0,+2\xi,0,0),\ (0,0,0,+\xi,+2\xi,0),\\&(0,+\xi,0,0,0,0),\ (0,-\xi,0,0,0,0).\end{aligned}\tag{16}$$

In total, to calculate all the independent SOECs, TOECs, and FOECs of a material with the cubic symmetry (point groups: 432, $4\bar{3}m$, and $m\bar{3}m$), our method requires 24 strain vectors (including the null vector for the reference state).

A material with the hexagonal symmetry (point groups: 622, $6mm$, $\bar{6}m2$, and $6/mmm$) has 5, 10, and 19 independent SOECs, TOECs, and FOECs, respectively [1, 39]. To calculate the 5 independent SOECs, we use the following 6 strain vectors:

$$\begin{aligned}&(0,0,0,0,0,0),\ (+\xi,0,0,0,0,0),\\&(-\xi,0,0,0,0,0),\ (0,0,0,+\xi,0,0),\\&(0,0,+\xi,0,0,0),\ (0,0,-\xi,0,0,0).\end{aligned}\tag{17}$$

To calculate the 10 independent TOECs, in addition to the strain vectors above, we need to account for the following 6 strain vectors:

$$\begin{aligned}&(0,+\xi,+\xi,0,0,0),\ (0,-\xi,+\xi,0,0,0),\\&(0,+\xi,-\xi,0,0,0),\ (0,-\xi,-\xi,0,0,0),\\&(0,+\xi,0,0,0,0),\ (0,-\xi,0,0,0,0).\end{aligned}\tag{18}$$

To obtain the 19 independent FOECs, we use the following 25 additional strain vectors:

$$\begin{aligned}&(+2\xi,0,0,0,0,0),\ (-2\xi,0,0,0,0,0),\\&(+2\xi,+\xi,0,0,0,0),\ (+2\xi,-\xi,0,0,0,0),\\&(-2\xi,+\xi,0,0,0,0),\ (-2\xi,-\xi,0,0,0,0),\\&(+\xi,0,+2\xi,0,0,0),\ (-\xi,0,+2\xi,0,0,0),\\&(+\xi,0,-2\xi,0,0,0),\ (-\xi,0,-2\xi,0,0,0),\\&(+\xi,0,0,+2\xi,0,0),\ (-\xi,0,0,+2\xi,0,0),\\&(+\xi,0,0,0,+2\xi,0),\ (-\xi,0,0,0,+2\xi,0),\\&(+\xi,0,0,0,0,+2\xi),\ (-\xi,0,0,0,0,+2\xi),\\&(0,+2\xi,+\xi,0,0,0),\ (0,+2\xi,-\xi,0,0,0),\\&(0,-2\xi,+\xi,0,0,0),\ (0,-2\xi,-\xi,0,0,0),\\&(0,0,+2\xi,0,0,0),\ (0,0,-2\xi,0,0,0),\\&(0,0,+\xi,+2\xi,0,0),\ (0,0,-\xi,+2\xi,0,0),\\&(0,0,0,+2\xi,0,0).\end{aligned}\tag{19}$$

In total, our method requires 37 strain vectors to calculate all the independent SOECs, TOECs, and FOECs of a material belonging to the hexagonal crystal system (point groups: 622, $6mm$, $\bar{6}m2$, and $6/mmm$).

2.3. Technical aspects of the method implementation

Our method to calculate linear and nonlinear elastic constants is implemented in codes that are part of the software package *xPK2x*, which is available under the GNU General Public License (Version 3) on GitHub [40]. This software package encompasses three Fortran modules, a Bash script, several example applications, and relevant documentation [40]. Our method relies on the availability of an external periodic DFT approach to optimize geometries and calculate the Cauchy stress tensor. To this end, the current version of *xPK2x* is designed to be compatible with the Quantum Espresso software package [41, 42]. For sake of clarity, here below we discuss the numerical operations and tasks implemented and carried out by the modules provided in *xPK2x*. We refer to the documentation available on GitHub [40] for additional information regarding installation and use of the programs.

The calculation of a set of elastic constants of a material requires, as a first step, to select a a periodic unit cell to describe the material in a reference state. The unit cell has a volume V and geometry $\boldsymbol{V}$:

$$\boldsymbol{V} = \begin{pmatrix} a_{1,x} & a_{2,x} & a_{3,x} \\ a_{1,y} & a_{2,y} & a_{3,y} \\ a_{1,z} & a_{2,z} & a_{3,z} \end{pmatrix}, \tag{20}$$

where $\vec{a}_1, \vec{a}_2, \vec{a}_3$ are the unit cell vectors. We remark that although the choice of the reference state and corresponding supercell is arbitrary, in this work we reports results obtained by considering primitive unit cells, and reference states yielding a zero static pressure. Then, given the list of elastic constants to be calculated, then next operation consists in determining the finite difference formulas to be

used, and therefore list of strain vectors required to generate the deformed configurations of the reference state. Geometry of the reference state and corresponding supercell, fractional coordinates of the atoms included in the supercell, list of six-dimensional strain vectors to generate the deformed configurations, and the strain parameter multiplying the strain vectors, all these are input parameters for the module *str2pk* of the software package *xPK2x* [40]. In particular, the numerical tasks implemented in the module *str2pk* are:

- Importing the geometry of the reference state and (fractional) coordinates of the atoms in the supercell (not necessarily a primitive unit cell), and reading the list of strain vectors. For each strain vector, which we can express in both the Voigt and tensorial forms as

$$\begin{aligned} \vec{\mu} &= (\xi_1, \xi_2, \xi_3, \xi_4, \xi_5, \xi_6) \\ \boldsymbol{\mu} &= \begin{pmatrix} \xi_1 & \xi_6/2 & \xi_5/2 \\ \xi_6/2 & \xi_2 & \xi_4/2 \\ \xi_5/2 & \xi_4/2 & \xi_3 \end{pmatrix}, \end{aligned} \tag{21}$$

  str2pk calculates the deformation gradient, $\boldsymbol{F}$, as described in Refs. [14, 31]. In particular, we first carry out the Cholesky decomposition of the following 3×3 matrix (see Eq. 1):

$$2\boldsymbol{\mu} + \mathbf{I} = \boldsymbol{D}\boldsymbol{D}^T. \tag{22}$$

  Then, a single value factorization of $\boldsymbol{D}$ is carried out, to obtain $\boldsymbol{D} = \boldsymbol{W}\boldsymbol{S}\boldsymbol{V}^T$, where $\boldsymbol{W}$ and $\boldsymbol{V}$ are unitary matrices, and $\boldsymbol{S}$ is the diagonal matrix of singular values. Finally, the rotation-free deformation gradient (right stretch tensor) is defined as $\boldsymbol{F} = \boldsymbol{V}\boldsymbol{S}\boldsymbol{V}^T$ ($\boldsymbol{R} = \boldsymbol{W}\boldsymbol{V}^T$ is the rotation tensor).

- Then, the deformation gradient, $\boldsymbol{F}$, is used to generate the unit cell of the deformed configuration by using Eq. 2. In particular, since we consider only homogeneous deformations of a material described by the use of a periodic unit cell $\boldsymbol{V}$, Eq. 2 assumes the form:

$$\boldsymbol{F} = \boldsymbol{V}'\boldsymbol{V}^{-1}, \tag{23}$$

  where $\boldsymbol{V}'$ is the 3×3 matrix defining the geometry of the material in the deformed state,

$$\boldsymbol{V}' = \begin{pmatrix} a'_{1,x} & a'_{2,x} & a'_{3,x} \\ a'_{1,y} & a'_{2,y} & a'_{3,y} \\ a'_{1,z} & a'_{2,z} & a'_{3,z} \end{pmatrix}. \tag{24}$$

  Thus, from Eq. 23, the deformed configuration is obtained as,

$$\boldsymbol{V}' = \boldsymbol{F}\boldsymbol{V}. \tag{25}$$

- Geometry and dimensions of the unit cells describing the deformed configurations, and (fractional) coordinates of the atoms in the unit cells, are printed out in text files.

The next step then consists in using a periodic DFT approach [41, 42] to optimize the geometry of each deformed configuration of the reference state, and calculate the corresponding Cauchy stress tensors, $\boldsymbol{\sigma}$. The list of Cauchy stress tensors are then supplied to a second module, *pk2ecs* [40], for the final calculation of the desired list of elastic constants. In detail, the numerical tasks implemented in this module are:

- For each deformed configuration $\boldsymbol{V}'$, Eq. 5 is used to calculate the PK2 stress tensor from the deformation gradient, $\boldsymbol{F}$, and the calculated Cauchy stress tensor, as follows:

$$\boldsymbol{P} = \frac{V'}{V}\boldsymbol{F}^{-1}\boldsymbol{\sigma}\boldsymbol{F}^{-T}, \tag{26}$$

  where V' is the volume of the deformed configuration.

- This operation is repeated for each strain vector, and the corresponding list of PK2 stress tensors is finally plugged into the finite difference formulas (Eqs. 8-11) to calculate the selected SOECs, TOECs, and FOECs.

We remark that the *xPK2x* package provides the lists of strain vectors required to calculate the independent SOECs, TOECs, and FOECs of a material with the cubic and hexagonal symmetry, and that the modules *str2pk* and *pk2ecs* are designed to be user-friendly for these classes of materials. In addition, we remark that the module *str2pk* can be used to generate any list of strained configurations for a reference state of a material with an arbitrary symmetry, and that the *xPK2x* package includes an additional module (*pk2open*) that can be easily adapted to the calculation of any elastic constant of the second, third, or fourth order. Instructions and examples about how to combine the modules *str2pk* and *pk2open* can be found on GitHub [40].

3. Results and discussion

3.1. Technical details of the DFT calculations

In this work, we use our method in combination with the "*pw.x*" code of the Quantum Espresso package [41, 42] to calculate the full set of independent SOECs, TOECs, and FOECs of diamond, silicon, aluminum, silver, gold, beryllium, and magnesium. In all DFT calculations, we use primitive unit cells, stringent convergence criteria (10^{-14} Ry for selfconsistency and 10^{-6} *a.u.* for forces), and unless stated otherwise, plane-wave energy cutoffs of 150 and 600 Ry to represent wavefunctions and electronic charge density, respectively. We underline that unless stated otherwise, all the elastic constants reported in this work are calculated using a strain parameter equal to 0.015.

For each material, we select a pseudopotential and an approximation of the exchange and correlation energy yielding SOECs in agreement with the experimental data. In particular, in case of Au we use a local density approximation [43], whereas for the rest of the materials we use

the Perdew-Burke-Ernzerhof parametrization [44] of the generalized gradient approximation.

To describe the diamond structure of C and Si, we use a uniform grid of 10×10×10 k-points to sample the Brillouin zone, and the ultrasoft psudopotentials *C.pbe-n-rrkjus_psl.1.0.0.UPF* and *Si.pbe-nl-rrkjus_psl.1.0.0.UPF* respectively. These pseudopotentials are part of the Quantum Espresso library [45]. To describe the *fcc* structure of Ag and Au, we use the ultrasoft pseudopotentials [45] *Ag.pbe-spn-rrkjus_psl.1.0.0.UPF* and *Au.pz-spn-rrkjus_psl.1.0.0.UPF*), respectively. In case of *fcc* Al, we use a norm-conserving psudopotential [46] generated by using the *fhi98PP* software [47] that was tested and used in a previous study [11]. To sample the Brillouin zone of the primitive unit cell of these three metals, we use a uniform grid of 25×25×25 k-points. In case of *hcp* Be and Mg, we use an ultrasoft [45] (*Be.pbe-n-rrkjus_psl.1.0.0.UPF*) and a norm-conserving [46] psudopotential, respectively. The latter psudopotential was generated by using the *fhi98PP* software [47] and was tested and used in a previous study [11]. To sample the Brillouin zones of Be and Mg, we use a grid of 20×20×14 k-points. With these technical details, we obtain the equilibrium lattice parameters at zero temperature reported in Table 1. These results are in agreement with experimental data.

Table 1: Lattice parameters (in Å) of the crystalline materials investigated in this study obtained from DFT calculations. Experimental values are also reported for comparison.

Crystal	Space group	a	c	Exp. (a/c)
C	$Fd\bar{3}m$	3.57	-	3.57 [7]
Si	$Fd\bar{3}m$	5.47	-	5.43 [48, 49]
Al	$Fm\bar{3}m$	4.07	-	4.03 [50]
Ag	$Fm\bar{3}m$	4.16	-	4.07 [50]
Au	$Fm\bar{3}m$	4.05	-	4.08 [51]
Be	$P6_3/mmc$	2.27	3.58	2.29/3.58 [52]
Mg	$P6_3/mmc$	3.24	5.28	3.18/5.15 [53]

3.2. Second- and third-order elastic constants

The independent SOECs and TOECs of crystals with the cubic and *hcp* structures calculated using our method are listed in Tables 2 and 3, respectively. These tables report also available experimental data and previous values calculated by using the conventional approach relying on fitting energy-strain or stress-strain curves [7–10, 12, 14]. Tables 2 and 3 show that our results are in overall good agreement with both experimental data and previous computational studies. It is to be noted that our elastic constants are calculated for a perfect monocrystalline material at zero temperature, whereas measurements of TOECs are typically carried out at finite temperature, by considering polycrystalline samples containing defects, which are known to affect the experimental data [8, 10]. These factors contribute to some extent to explain the small differences between our results and the experimental data. We also underline that, as discussed in Ref. [56], another possible source of discrepancy between calculations and experiments may stem from approximations in in the data analysis. As shown in Ref. [56], this is certainly the case for $C^{(3)}_{123}$ of diamond, whose value after accounting for higher order effects has been estimated to be 640 GPa, rather than 2100 GPa as reported in Ref. [10].

As for the differences between our results and those of previous computational studies, we argue that these stem mainly from the following two reasons. One, the technical aspects of the DFT calculations, namely plane-wave energy cutoffs, pseudopotentials, convergence thresholds, and the exchange and correlation energy functional. Two, the details of the fitting procedure used to deduce the full set of independent linear and nonlinear elastic constants [13]. To corroborate this last argument, and at the same time, to demonstrate the validity of our method and results, we adopt the conventional approach based on fitting an energy-strain curve to calculate the selected second- and higher-order elastic constants of Si. In particular, we consider the following three deformation vectors:

$$(+\xi,0,0,0,0,0),\ (+\xi,+\xi,0,0,0,0),$$
$$(+\xi,-\xi,0,0,0,0), \tag{27}$$

and we generate a set of deformed configurations by varying the strain parameter ξ from -0.2 to 0.3. We then use fourth-order polynomial functions to fit the resulting curves and obtain the set of second-, third-, and fourth-order elastic constants governing the changes of the energy density versus the strain parameter [8]. In case of the uniaxial deformation, we use a fifth-order polynomial to also deduce the value of $C^{(5)}_{11111}$. Calculated energies and fitting functions are shown in Fig. 1, where for clarity we report only the results obtained for the first two deformation modes in Eq. 27. Overall, our fitting procedure yields the following results: $C^{(2)}_{11}$=153 GPa, $C^{(2)}_{12}$=57 GPa, $C^{(3)}_{111}$=-730 GPa, $C^{(3)}_{112}$=-541 GPa, $C^{(4)}_{1111}$=2555 GPa, $C^{(4)}_{1112}$=2157 GPa, $C^{(4)}_{1122}$=1874 GPa, and $C^{(5)}_{11111}$=-10493 GPa of Si (Fig. 1). These values are in overall good agreement with the elastic constants computed by using the present method reported in Tables 2 and 4. We remark that, as thoroughly discussed in Ref. [56], the order of the polynomials used to fit the energy curves influences the results of this operation. In the present case, we find that fifth- and sixth-order polynomial functions yield, for example, values for $C^{(3)}_{112}$ and $C^{(4)}_{1122}$ equal to about -437 GPa and 2114 GPa, respectively in better and worse agreement with the values in Tables 2 and 4.

3.3. Fourth-order elastic constants

To assess the accuracy of our method, we carry out convergence tests. In particular, we calculate the values of selected FOECs of *fcc* Al for increasing values of the strain parameter (ξ), as well as by considering DFT calculations of increasing precision (Fig. 2). The results of these calculations show that FOECs converge rapidly for increasing

Table 2: Independent SOECs and TOECs (in GPa) of cubic diamond, silicon, aluminum, silver, and gold calculated using the method presented in this work. For each material, the first row shows our results, the second row reports experimental data, and the remaining rows show previous results obtained by using the conventional approach based on fitting energy-strain or stress-strain data points.

Crystal		$C_{11}^{(2)}$	$C_{12}^{(2)}$	$C_{44}^{(2)}$	$C_{111}^{(3)}$	$C_{112}^{(3)}$	$C_{123}^{(3)}$	$C_{144}^{(3)}$	$C_{155}^{(3)}$	$C_{456}^{(3)}$
C	This work	1054	124	559	-5942	-1621	614	-200	-2773	-1152
	Exp. [10]	1082	125	579	-7750	-2220	2100	-1780	-2800	-30
	Ref. [11]	1037	120	552	-5876	-1593	618	-197	-2739	-1111
Si	This work	153	57	75	-751	-423	-78	16	-294	-59
	Exp. [28]	166	64	80	-795	-445	-75	15	-310	-86
	Ref. [11]	142	51	72	-744	-393	-59	4	-297	-59
	Ref. [13]	152	59	78	-653	-456	-96	23	-304	-7
Al	This work	103	55	31	-1095	-330	44	-35	-357	-14
	Exp. [27]	107	60	28	-1076	-315	36	-23	-340	-30
	Ref. [11]	108	59	33	-1100	-371	104	39	-421	-22
Ag	This work	107	79	42	-962	-566	-89	-9	-444	19
	Exp. [29, 30]	124	94	46	-843	-529	189	56	-637	83
	Ref. [8]	161	119	58	-1012	-975	162	80	-759	53
Au	This work	207	179	35	-1985	-1177	-373	-63	-749	63
	Exp. [29, 30]	192	163	42	-1729	-922	-233	-13	-648	-12
	Ref. [8]	202	174	38	-2023	-1266	-263	-63	-930	54
	Ref. [15]	151	126	28	-1438	-875	-550	-66	-469	16

Table 3: Independent SOECs and TOECs (in GPa) of *hcp* beryllium and magnesium. For each crystal, the first row shows our results, the second row reports experimental data, and the remaining rows show previous results obtained by using the conventional approach.

	$C_{11}^{(2)}$	$C_{12}^{(2)}$	$C_{13}^{(2)}$	$C_{33}^{(2)}$	$C_{44}^{(2)}$	$C_{111}^{(3)}$	$C_{112}^{(3)}$	$C_{113}^{(3)}$	$C_{123}^{(3)}$	$C_{133}^{(3)}$	$C_{144}^{(3)}$	$C_{155}^{(3)}$	$C_{222}^{(3)}$	$C_{333}^{(3)}$	$C_{344}^{(3)}$
Be															
This work	275	40	30	309	141	-3160	211	33	-170	52	-139	-344	-2414	-3826	-948
Exp. [54]	294	27	14	357	162	–	–	–	–	–	–	–	–	–	–
Ref. [55]	333	16	5	392	171	-5093	1187	707	-87	-838	-435	-475	-2845	-2048	-489
Mg															
This work	54	23	17	58	15	-702	-31	-1	-43	-101	-21	-72	-546	-619	-155
Exp. [26]	59	26	–	62	16	-663	-178	30	-76	-86	-30	-58	-864	-726	-193
Ref. [11]	58	24	19	62	16	-602	-190	4	-55	-107	-60	-50	-762	-657	-163
Ref. [31]	68	28	20	70	18	-784	-241	97	-46	-116	-52	-29	-1081	-554	-154

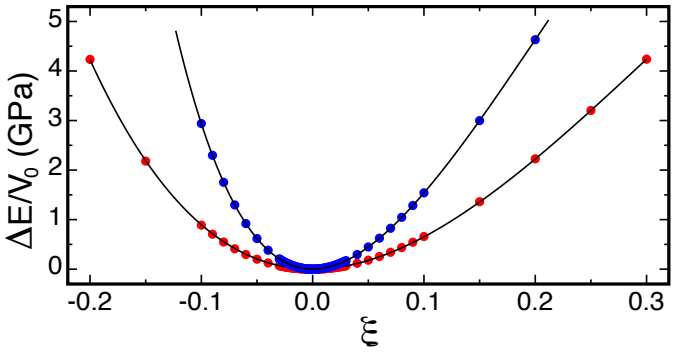

Figure 1: Energy density of cubic Si relative to that one of the reference state versus strain parameter. The solid black lines show the higher order polynomial functions fitting the data (discs) calculated from DFT. The red and blue discs show results obtained by deforming the reference state using strain vectors $(+\xi, 0, 0, 0, 0, 0)$ and $(+\xi, +\xi, 0, 0, 0, 0)$, respectively.

values of both the k-points grid density and plane-wave energy cutoff. Also, these calculations show that FOECs are sensitive to the value of the strain parameter used to generate the deformed configurations of a reference state. In particular, Fig. 2 shows that although several FOECs fluctuate significantly for strain parameters smaller than 0.0075, all the independent FOECs converge and plateau for strain parameters larger than 0.01. We also carry out similar convergence tests for all the independent SOECs and TOECs of Al. These calculations show that similarly to FOECs, SOECs and TOECs converge rapidly with both the k-points grid density and plane-wave energy cutoff. In contrast, these calculations show that SOECs and TOECs are less sensitive than FOECs to the value of the strain parameter, plateauing to the converged values for strain parameters equal or larger than 0.005.

For completeness, we carry out calculations to assess the impact of the accuracy of the finite difference formulas used to calculate elastic constants. In particular, we

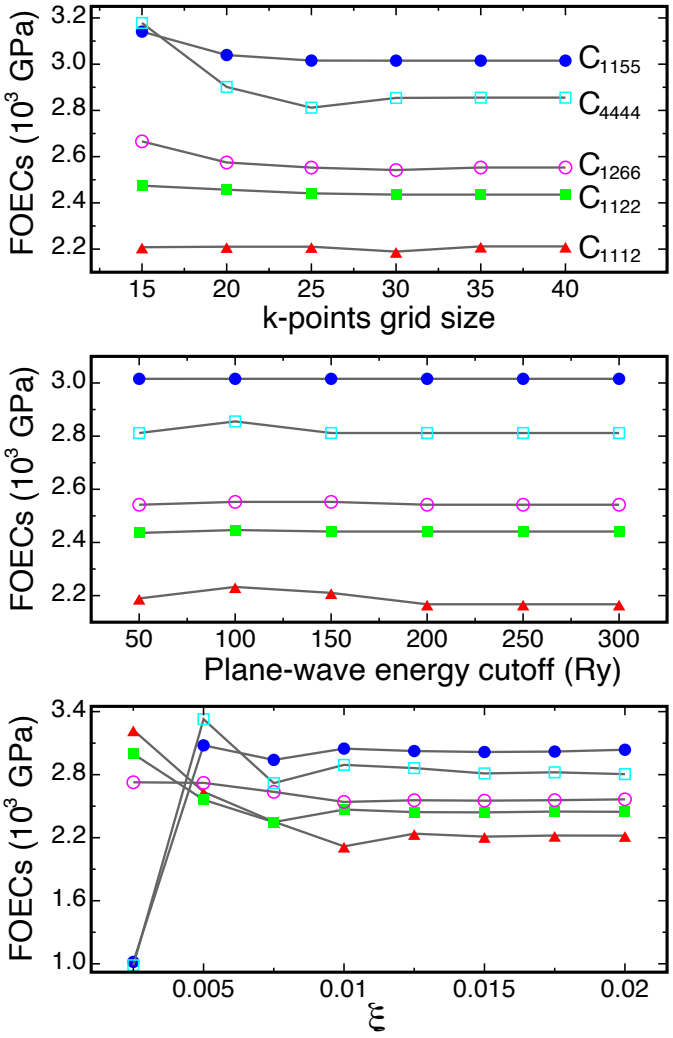

Figure 2: Selected FOECs of *fcc* Al calculated with the present method by using DFT calculations of increasing precision and increasing values of the strain parameter. Top panel, FOECs are obtained from DFT calculations using uniform grids of k-points of increasing density, and fixed values of 150 Ry and 0.015 for the plane-wave energy cutoff and strain parameter, respectively. Middle panel, FOECs are obtained from DFT calculations using increasing values of the plane-wave energy cutoff to represent wavefunctions, and a fixed 25×25×25 grid of k-points and a strain parameter of 0.015. Bottom panel, FOECs are calculated by using Eq. 11 with increasing values of the strain parameter, and DFT calculations using a plane-wave energy cutoff of 150 Ry and a 25×25×25 grid of k-points. Calculated FOECs are shown by using red filled triangles ($C^{(4)}_{1112}$), green filled squares ($C^{(4)}_{1122}$), blue filled circles ($C^{(4)}_{1155}$), magenta open circles ($C^{(4)}_{1266}$), and cyan open squares ($C^{(4)}_{4444}$).

calculate all the SOECs and selected TOECs ($C^{(3)}_{111}$, $C^{(3)}_{112}$, and $C^{(3)}_{144}$) and FOECs ($C^{(4)}_{1111}$, $C^{(4)}_{1112}$, and $C^{(4)}_{4444}$) of Al by using central difference formulas with 4^{th}-order accuracy. The results of these calculations are compared to the values in Tables 2 and 4, which are obtained by using the central difference formulas with 2^{th}-order accuracy shown in Eqs. 8, 9, and 11. These comparisons show that the two sets of elastic constants are practically identical, thereby demonstrating that the truncation errors resulting from the use of the finite difference formulas in Eqs. 8-11 are small, and hence that the results presented on our work are accurate and reliable. Overall, we underline that all our calculations to test accuracy and validity show that the main source of inaccuracy of our method lies in the numerical precision of the strain tensor computed by using a DFT approach employing plane-wave basis sets. To reduce the impact of these errors, we adopt the following solutions: using (i) values for the energy cutoffs that are larger than the minimal suggested ones, and (ii) stringent convergence criteria.

Table 4 reports calculated values of FOECs of diamond, Si, Al, Ag, and Au. To the best of our knowledge, experimental data for these coefficients are missing from literature. Values of FOECs obtained using the present method are in reasonable agreement with previous results obtained by employing the conventional approach. We remark that our method yields results in excellent agreement with FOECs obtained by fitting energy-strain curves. In fact, as discussed above, these two methods yield values of $C^{(4)}_{1111}$ for Si equal to 2586 and 2555 GPa, respectively. Therefore, once again we are inclined to attribute the differences between our results and previous calculations [8, 10, 13, 15] to both different technicalities of the DFT calculations and/or details of the fitting procedure.

It is interesting to notice that Hiki *et al.* [30, 57] suggested that "*the contribution from the closed-shell repulsive interaction between nearest-neighbor ions becomes predominant for determining the higher order elastic constants for materials with markedly overlapped closed shells*", and therefore that FOECs of metals such as Ag and Au should obey the following approximate relationships:

$$\begin{aligned} &C^{(4)}_{1111} = 2C^{(4)}_{1112} = 2C^{(4)}_{1122} = 2C^{(4)}_{1155} = 2C^{(4)}_{1266} = 2C^{(4)}_{4444} \\ &C^{(4)}_{1123} = C^{(4)}_{1144} = C^{(4)}_{1255} = C^{(4)}_{1456} = C^{(4)}_{4455} = 0. \end{aligned} \tag{28}$$

Using our calculated values for Ag in Table 4, we find $C^{(4)}_{1111}/C^{(4)}_{1112}$=1.9, $C^{(4)}_{1111}/C^{(4)}_{1122}$=2.0, $C^{(4)}_{1111}/C^{(4)}_{1155}$=2.2, $C^{(4)}_{1111}/C^{(4)}_{1266}$=2.2, and $C^{(4)}_{1111}/C^{(4)}_{4444}$=2.3, i.e. all values close to 2.0, whereas the remaining FOECs are much smaller than $C^{(4)}_{1111}$ and thus negligible. This result not only corroborates the argument put forward by Hiki *et al.* [30, 57], but it further validates the correctness of our method.

Existing methods based on fitting energy-strain or stress-strain curves become cumbersome and difficult to apply in case of materials with a symmetry lower than the cubic. In contrast, our method is easily applicable to materials of any symmetry, and the computational workload increases only moderately as the symmetry of the material decreases. Here, to demonstrate the potential of the present method, we calculate the independent FOECs

of *hcp* Be and Mg. The results of these calculations are shown in Table 5. To the best of our knowledge, FOECs of these two materials have so far neither been measured nor calculated.

3.4. Potential application of our method

Fourth- and higher-order elastic constants describe the elastic response of a material subjected to large deformations [8, 12, 14, 36, 37]. Knowledge of these higher-order elastic coefficients can be thus used to predict, within the context of a nonlinear elasticity theory treatment, both the strain response and SOECs of a material subjected to an external pressure (or stress). In this section, we show that indeed SOECs, TOECs, and most importantly, FOECs, can be used for this purpose, and that FOECs expand the predictive power of the numerical framework relying on nonlinear elasticity theory to larger intervals of strain and pressures. Here we show the results obtained for *fcc* Si and *hcp* Mg.

We use both DFT calculations and nonlinear elasticity theory to calculate the volume, $V(p)$, and bulk modulus, $B_0(p)$, of Si and Mg at zero temperature over a finite interval of pressures. First, we use variable-cell optimization calculations [41, 42] and the finite difference formulas in Eq. 8 to calculate from DFT, first the volume, and then the SOECs of Si and Mg at a pressure p. To calculate $B_0(p)$ of *fcc* Si and *hcp* Mg, we use the formulas [38, 58, 59]

$$B_0(p) = \frac{C_{11}^{(2)} + 2C_{12}^{(2)} + p}{3} \tag{29}$$

and

$$B_0(p) = \frac{2(C_{11}^{(2)} + C_{12}^{(2)}) + C_{33}^{(2)} + 4C_{13}^{(2)} + 3p}{9}, \tag{30}$$

respectively. Second, we calculate the same quantities, $V(p)$ and $B_0(p)$, within the context of nonlinear elasticity theory by employing elastic coefficients calculated with the present method (Tables 2-5). We underline that these coefficients are obtained by considering a reference state yielding a zero static pressure at zero temperature, V_0. Thus, for each value of the pressure p, we use a self-consistent variational approach to solve Eqs. 5 and 6 and find the strain required to deform the reference state and obtain a configuration for the material, $V(p)$, yielding the selected pressure [4]. After determining the geometry of the material at p, we proceed to calculate the SOECs and therefore the bulk modulus $B_0(p)$ using the same approach relying on the finite difference formulas in Eq. 8. However, in this case, the Cauchy and hence PK2 stress tensor resulting from a deformation of the state $V(p)$ is not calculated explicitly from DFT, but instead it is again derived from Eqs. 5 and 6 as outlined in the following diagram:

$$\begin{aligned} V(p) \xrightarrow{\tilde{\boldsymbol{\mu}}} \tilde{\boldsymbol{F}}, \tilde{V} \xrightarrow{V_0} \boldsymbol{\mu}, \boldsymbol{F} \xrightarrow{\text{Eq.[6]}} \boldsymbol{P}(\boldsymbol{\mu}) \xrightarrow{\boldsymbol{F}} \dots \\ \dots \xrightarrow{\boldsymbol{F}} \boldsymbol{\sigma}(\boldsymbol{\mu}) = \tilde{\boldsymbol{\sigma}}(\tilde{\boldsymbol{\mu}}) \xrightarrow{\tilde{\boldsymbol{F}}} \tilde{\boldsymbol{P}}(\tilde{\boldsymbol{\mu}}), \end{aligned} \tag{31}$$

where $\tilde{\boldsymbol{\mu}}$ and $\tilde{\boldsymbol{F}}$ are the Lagrangian strain and corresponding deformation gradient mapping $V(p)$ to one of its deformed states, $\tilde{V}$, whereas $\boldsymbol{\mu}$ and $\boldsymbol{F}$ are the strain and deformation gradient mapping the reference state at zero pressure, V_0, to $\tilde{V}$. Thanks to this last correspondence, Eq. 6 can be used to extrapolate the value of the PK2 stress tensor in $\tilde{V}$ resulting from the deformation of $V(p)$, and Eq. 5 can be used to, first, calculate the Cauchy stress, $\boldsymbol{\sigma}(\boldsymbol{\mu}) = \tilde{\boldsymbol{\sigma}}(\tilde{\boldsymbol{\mu}})$, and then the PK2 stress tensor resulting from the deformation of $V(p)$, which is needed to calculate its SOECs.

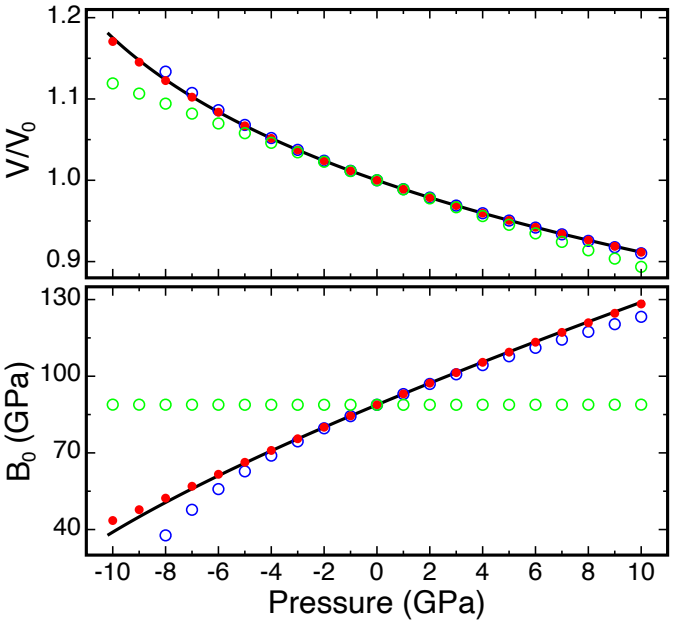

Figure 3: Volume (top) relative to that one at zero pressure and bulk modulus (bottom) of cubic Si versus pressure. Black solid line shows results obtained from DFT calculations, whereas discs and circles show results obtained from nonlinear elasticity theory: green circles, blue circles, and red discs show results obtained by considering only SOECs, SOECS and TOECs, and all the elastic constants up to FOECs, respectively.

The results of these two sets of calculations are compared in Figs. 3 and 4 for Si and Mg, respectively. These comparisons show, as expected, that the formalism relying on nonlinear elasticity theory yields results that agree with those obtained from DFT over larger intervals of pressure for increasing the order of the truncation in Eq. 6, i.e. considering the higher-order elastic constants. In particular, while in case of the equation of state $V(p)$, a good agreement is already reached by considering only SOECs and TOECs, in case of $B_0(p)$, the inclusion of FOECs in Eq. 6 is necessary to achieve an excellent agreement over the full intervals of pressures.

4. Conclusion

We presented a method to calculate second-, third-, and fourth-order elastic constants of crystals with the cubic

Table 4: Independent FOECs (in GPa) of cubic diamond, silicon, aluminum, silver, and gold obtained by using the present method. Our results are compared to values calculated by employing the conventional approach relying on fitting energy-strain curves.

		$C^{(4)}_{1111}$	$C^{(4)}_{1112}$	$C^{(4)}_{1122}$	$C^{(4)}_{1123}$	$C^{(4)}_{1144}$	$C^{(4)}_{1155}$	$C^{(4)}_{1255}$	$C^{(4)}_{1266}$	$C^{(4)}_{1456}$	$C^{(4)}_{4444}$	$C^{(4)}_{4455}$
C	This work	36057	9864	6768	-519	-1747	12628	284	9662	1236	12926	1169
	Ref. [10]	26687	9459	6074	-425	-1385	10741	-264	8192	487	11328	528
Si	This work	2586	2112	1885	576	-671	833	-422	742	-46	1268	-2
	Ref. [13]	613	2401	1275	1053	5071	4050	-2728	-514	66	-2553	-577
Al	This work	10102	2210	2441	-609	-68	3016	159	2553	224	2812	180
	Ref. [8]	9916	2656	3708	-1000	-578	3554	-91	4309	148	3329	127
Ag	This work	8346	4429	4204	333	99	3735	21	3813	-39	3638	-86
	Ref. [8]	13694	7115	6652	-387	-154	5295	3	6718	-196	5416	-75
Au	This work	17113	8114	8814	874	860	7462	-634	7372	-257	8258	-61
	Ref. [8]	17951	8729	9033	416	691	7774	-752	9402	-170	8352	15
	Ref. [15]	10094	8280	8402	1507	235	5549	-1534	8252	2	3640	-5763

Table 5: Independent FOECs (in GPa) of *hcp* beryllium and magnesium calculated by using the present method.

	$C^{(4)}_{1111}$	$C^{(4)}_{1112}$	$C^{(4)}_{1113}$	$C^{(4)}_{1122}$	$C^{(4)}_{1133}$	$C^{(4)}_{1123}$	$C^{(4)}_{1144}$	$C^{(4)}_{1155}$	$C^{(4)}_{1166}$	$C^{(4)}_{1223}$
Be	32466	-3	358	-3529	-3721	881	-1902	-1342	-2880	1770
Mg	8638	-79	-243	119	-57	-47	-69	-40	-188	266
	$C^{(4)}_{1233}$	$C^{(4)}_{1244}$	$C^{(4)}_{1255}$	$C^{(4)}_{1333}$	$C^{(4)}_{1344}$	$C^{(4)}_{1355}$	$C^{(4)}_{3333}$	$C^{(4)}_{3344}$	$C^{(4)}_{4444}$	
Be	-2113	3838	18	9934	229	1629	9986	8380	-5202	
Mg	347	353	-30	828	392	240	5684	1402	-1073	

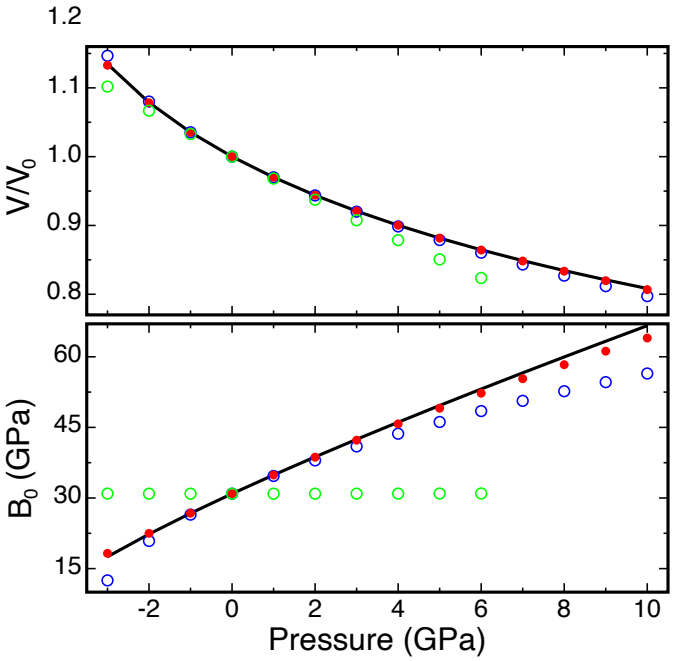

Figure 4: Same as Fig. 3 for *hcp* Mg

and hexagonal symmetry. This *first-principles* method relies on the numerical differentiation of the second Piola-Kirchhoff stress tensor and a list of strained configurations of a reference state for a material. In particular, the number of configurations required to calculate the independent elastic constants up to the fourth order is 24 and 37 for a crystal with the cubic and hexagonal symmetry, respectively. Although here we have shown applications to materials with the cubic and hexagonal symmetry, our method has general applicability as, regardless of symmetry, each elastic constant of any order can be calculated independently by carrying out several DFT calculations. This important aspect is what differentiates our method from conventional approaches based on fitting energy-strain or stress-strain curves.

To validate our method, here we calculated the elastic constants up to the fourth order of five and two materials with the *fcc* and *hcp* structures, respectively. Comparisons of our results with available experimental data and previous calculations show that our method is reliable and accurate. We have also used a formalism based on nonlinear elasticity theory to predict the equation of state and elastic properties of a material over finite intervals of pressure. This formalism requires as input parameters linear and nonlinear elastic constants of a material in a reference state, and its predictive power improves as higher-order elastic constants are accounted for. Our method is flexible and can be extended to the calculation of elastic constants of the fifth or higher order of a material with an arbitrary symmetry. Therefore, the present method has the potential to enhance the capabilities of the aforementioned formalism based on nonlinear elasticity theory to predict, for example, thermoelastic behaviors [4], the occurrence of solid phase transitions [13], and values of ideal yield strengths [13].

5. Acknowledgements

This work is supported by the National Science Foundation (NSF), Award No. DMR-2036176. We acknowledge the support of the CUNY High Performance Computing Center, the PSC-CUNY grants 62651-0050 and 63913-0051.

References

[1] J. Clayton, Nonlinear Mechanics of Crystals, Springer, Dordrecht, 2011.

[2] M. de Jong, W. Chen, T. Angsten, A. Jain, R. Notestine, A. Gamst, M. Sluiter, C. K. Ande, S. van der Zwaag, J. J. Plata, C. Toher, S. Curtarolo, G. Ceder, K. A. Persson, M. Asta, Charting the complete elastic properties of inorganic crystalline compounds, Sci. Data 2 (2015) 150009.

[3] D. Cuffari, A. Bongiorno, Calculation of mode grüneisen parameters made simple, Phys. Rev. Lett. 124 (2020) 215501.

[4] A. Bakare, A. Bongiorno, Enhancing efficiency and scope of first-principles quasiharmonic approximation methods through the calculation of third-order elastic constants, Phys. Rev. Materials 6 (2022) 043803.

[5] Z. P. Chang, G. R. Barsch, Nonlinear pressure dependence of elastic constants and fourth-order elastic constants of cesium halides, Phys. Rev. Lett. 19 (1967) 1381–1382.

[6] J. M. Lang, Y. M. Gupta, Experimental determination of third-order elastic constants of diamond, Phys. Rev. Lett. 106 (2011) 125502.

[7] O. H. Nielsen, R. M. Martin, Stresses in semiconductors: Ab initio calculations on si, ge, and gaas, Phys. Rev. B 32 (1985) 3792–3805.

[8] H. Wang, M. Li, Ab initio calculations of second-, third-, and fourth-order elastic constants for single crystals, Phys. Rev. B 79 (2009) 224102.

[9] Y. K. Vekilov, O. M. Krasilnikov, A. V. Lugovskoy, Y. E. Lozovik, Higher-order elastic constants and megabar pressure effects of bcc tungsten: Ab initio calculations, Phys. Rev. B 94 (2016) 104114.

[10] A. V. Telichko, S. V. Erohin, G. M. Kvashnin, P. B. Sorokin, B. P. Sorokin, V. D. Blank, Diamond's third-order elastic constants: ab initio calculations and experimental investigation, J. Mater. Sci. 52 (2017) 3447.

[11] T. Cao, D. Cuffari, A. Bongiorno, First-principles calculation of third-order elastic constants via numerical differentiation of the second piola-kirchhoff stress tensor, Phys. Rev. Lett. 121 (2018) 216001.

[12] O. M. Krasilnikov, Y. K. Vekilov, Fourth-order elastic moduli of polycrystals, Phys. Rev. B 100 (2019) 134107.

[13] H. Chen, N. A. Zarkevich, V. I. Levitas, D. D. Johnson, X. Zhang, Fifth-degree elastic energy for predictive continuum stress–strain relations and elastic instabilities under large strain and complex loading in silicon, npj Comp. Mater. 6 (2020) 115.

[14] S. P. Łepkowski, First-principles calculation of higher-order elastic constants using exact deformation-gradient tensors, Phys. Rev. B 102 (2020) 134116.

[15] M. Liao, Y. Liu, F. Zhou, T. Han, D. Yang, N. Qu, Z. Lai, Z.-K. Liu, J. Zhu, A high-efficient strain-stress method for calculating higher-order elastic constants from first-principles, Comput. Phys. Commun. 280 (2022) 108478.

[16] G. A. Saunders, H. B. Senin, H. A. A. Sidek, J. Pelzl, Third-order elastic constants, vibrational anharmonicity, and the invar behavior of the $fe_{72}pt_{28}$ alloy, Phys. Rev. B 48 (1993) 15801–15806.

[17] R. N. Thurston, K. Brugger, Third-order elastic constants and the velocity of small amplitude elastic waves in homogeneously stressed media, Phys. Rev. 135 (1964) 16043.

[18] J. Philip, M. A. Breazeale, Third-order elastic constants and grüneisen parameters of silicon and germanium between 3 and 300^ok, J. Appl. Phys. 54 (1983) 752.

[19] J. M. Ziman, Electrons and Phonons, Clarendon, Oxford, 1960.

[20] Y. Hiki, Higher order elastic constants of solids, Ann. Rev. Mater. Sci. 11 (1981) 51–73.

[21] D. C. Wallace, Thermodynamics of Crystals, Dover Publications, New York, USA, 1998.

[22] J. Clayton, R. Kraft, R. Leavy, Mesoscale modeling of nonlinear elasticity and fracture in ceramic polycrystals under dynamic shear and compression, Int. J. Solids Struct. 49 (2012) 2686.

[23] K. Brugger, Pure modes for elastic waves in crystals, J. Appl. Phys. 36 (1965) 759.

[24] M. H. Grimsditch, E. Anastassakis, M. Cardona, Effect of uniaxial stress on the zone-center optical phonon of diamond, Phys. Rev. B 18 (1978) 901–904.

[25] A. S. Johal, D. J. Dunstan, Reappraisal of experimental values of third-order elastic constants of some cubic semiconductors and metals, Phys. Rev. B 73 (2006) 024106.

[26] E. R. Naimon, Third-order elastic constants of magnesium. i. experimental, Phys. Rev. B 4 (1971) 4291–4296.

[27] J. F. Thomas, Third-order elastic constants of aluminum, Phys. Rev. 175 (1968) 955–962.

[28] J. J. Hall, Electronic effects in the elastic constants of n-type silicon, Phys. Rev. 161 (1967) 756–761.

[29] J. R. Neighbours, G. A. Alers, Elastic constants of silver and gold, Phys. Rev. 111 (1958) 707–712.

[30] Y. Hiki, A. V. Granato, Anharmonicity in noble metals; higher order elastic constants, Phys. Rev. 144 (1966) 411–419.

[31] M. Liao, Y. Liu, S.-L. Shang, F. Zhou, N. Qu, Y. Chen, Z. Lai, Z.-K. Liu, J. Zhu, Elastic3rd: A tool for calculating third-order elastic constants from first-principles calculations, Comput. Phys. Commun. 261 (2021) 107777.

[32] E. R. Naimon, T. Suzuki, A. V. Granato, Third-order elastic constants of magnesium. ii. theoretical, Phys. Rev. B 4 (1971) 4297–4305.

[33] J. Zhao, J. M. Winey, Y. M. Gupta, First-principles calculations of second- and third-order elastic constants for single crystals of arbitrary symmetry, Phys. Rev. B 75 (2007) 094105.

[34] E. Cadelano, P. L. Palla, S. Giordano, L. Colombo, Nonlinear elasticity of monolayer graphene, Phys. Rev. Lett. 102 (2009) 235502.

[35] A. Hmiel, J. M. Winey, Y. M. Gupta, M. P. Desjarlais, Nonlinear elastic response of strong solids: First-principles calculations of the third-order elastic constants of diamond, Phys. Rev. B 93 (2016) 174113.

[36] T. S. G. Krishnamurty, Fourth-order elastic coefficients in crystals, Acta Cryst. 16 (1963) 839.

[37] P. B. Ghate, Fourth-order elastic coefficients, J. Appl. Phys. 35 (1964) 337.

[38] D. C. Wallace, Thermoelasticity of stressed materials and comparison of various elastic constants, Phys. Rev. 162 (1967) 776–789.

[39] X. Markenscoff, The independent fourth-order elastic coefficients for the trigonal and hexagonal symmetry classes, J. Appl. Phys. 50 (1979) 1325–1327.

[40] A. Pandit, A. Bongiorno, A software package to calculate elastic constants up to the fourth order from first principles, (https://github.com/abongiox/xPK2x).

[41] P. Giannozzi, S. Baroni, N. Bonini, M. Calandra, R. Car, C. Cavazzoni, D. Ceresoli, G. L. Chiarotti, M. Cococcioni, I. Dabo, A. Dal Corso, S. de Gironcoli, S. Fabris, G. Fratesi, R. Gebauer, U. Gerstmann, C. Gougoussis, A. Kokalj, M. Lazzeri, L. Martin-Samos, N. Marzari, F. Mauri, R. Mazzarello, S. Paolini, A. Pasquarello, L. Paulatto, C. Sbraccia, S. Scandolo, G. Sclauzero, A. P. Seitsonen, A. Smogunov, P. Umari, R. M. Wentzcovitch, Quantum espresso: a modular and open-source software project for quantum simulations of materials, J. Phys.: Cond. Matter 21 (39) (2009) 395502.

[42] P. Giannozzi, O. Andreussi, T. Brumme, O. Bunau, M. B. Nardelli, M. Calandra, R. Car, C. Cavazzoni, D. Ceresoli, M. Cococcioni, N. Colonna, I. Carnimeo, A. D. Corso, S. de Gironcoli, P. Delugas, R. A. DiStasio, A. Ferretti, A. Floris, G. Fratesi, G. Fugallo, R. Gebauer, U. Gerstmann, F. Giustino, T. Gorni, J. Jia, M. Kawamura, H.-Y. Ko, A. Kokalj, E. Küçükbenli, M. Lazzeri, M. Marsili, N. Marzari, F. Mauri, N. L. Nguyen, H.-V. Nguyen, A. O. de-la Roza, L. Paulatto, S. Poncé, D. Rocca, R. Sabatini, B. Santra, M. Schlipf, A. P. Seitsonen, A. Smogunov, I. Timrov, T. Thonhauser, P. Umari, N. Vast, X. Wu, S. Baroni, Advanced capabilities for materials modelling with quantum ESPRESSO, J. Phys.: Cond. Matter 29 (2017) 465901.

[43] J. P. Perdew, A. Zunger, Self-interaction correction to density-functional approximations for many-electron systems, Phys.

Rev. B 23 (1981) 5048–5079.
[44] J. P. Perdew, K. Burke, M. Ernzerhof, Generalized gradient approximation made simple, Phys. Rev. Lett. 77 (1996) 3865–3868.
[45] A. D. Corso, The pslibrary pseudopotential library, (https://github.com/dalcorso/pslibrary).
[46] N. Troullier, J. L. Martins, Efficient pseudopotentials for plane-wave calculations, Phys. Rev. B 43 (1991) 1993–2006.
[47] M. Fuchs, M. Scheffler, Ab initio pseudopotentials for electronic structure calculations of poly-atomic systems using density-functional theory, Comput. Phys. Commun. 119 (1999) 67–98.
[48] M. E. Straumanis, P. Boregeaud, W. J. James, Perfection of the lattice of dislocation-free silicon, studied by the lattice-constant and density method, J. Appl. Phys. 32 (1961) 1382.
[49] J. Donohue, The Structures of the Elements, Wiley, New York, 1974.
[50] M. E. Straumanis, C. L. Woodard, Lattice parameters and thermal expansion coefficients of ai, ag and mo at low temperatures. comparison with dilatometric data*, Acta Cryst. A27 (1971) 549.
[51] Y. Akahama, H. Kawamura, A. K. Singh, A comparison of volume compressions of silver and gold up to 150 gpa, J. Appl. Phys. 95 (2004) 4767.
[52] K. Mackay, N. Hill, Lattice parameter and hardness measurements on high purity beryllium, J. Nucl. Mater. 8 (2) (1963) 263–264.
[53] D. Errandonea, Y. Meng, D. Häusermann, T. Uchida, Study of the phase transformations and equation of state of magnesium by synchrotron x-ray diffraction, J. Phys.: Cond. Matter 15 (8) (2003) 1277.
[54] A. Migliori, H. Ledbetter, D. J. Thoma, T. W. Darling, Beryllium's monocrystal and polycrystal elastic constants, J. Appl. Phys. 95 (5) (2004) 2436–2440.
[55] M. de Jong, I. Winter, D. C. Chrzan, M. Asta, Ideal strength and ductility in metals from second- and third-order elastic constants, Phys. Rev. B 96 (2017) 014105.
[56] M. Liao, Y. Liu, Y. Wang, F. Zhou, N. Qu, T. Han, D. Yang, Z. Lai, Z.-K. Liu, J. Zhu, Revisiting the third-order elastic constants of diamond: The higher-order effect, Diam. Relat. Mater. 117 (2021) 108490.
[57] Y. Hiki, J. F. Thomas, A. V. Granato, Anharmonicity in noble metals: Some thermal properties, Phys. Rev. 153 (1967) 764–771.
[58] M. Jafari, N. Zarifi, M. Nobakhti, A. Jahandoost, M. Lame, Pseudopotential calculation of the bulk modulus and phonon dispersion of the bcc and hcp structures of titanium, Phys. Scr. 83 (2011) 065603.
[59] J.-N. Yuan, Y. Cheng, X.-Q. Zhang, X.-R. Chen, L.-C. Cai, First-principles study of electronic and elastic properties of hexagonal layered crystal mos2 under pressure, Z. Naturforsch. A 70 (2015) 529.